

PACS numbers: 42.55.Wd; 42.65.Ky; 42.65.Re; 42.81.Dp
DOI: 10.1070/QE2013v043n03ABEH015131

Nonlinear frequency up-conversion of femtosecond pulses from an erbium fibre laser to the range of 0.8–1 μm in silica fibres

E.A. Anashkina, A.V. Andrianov, A.V. Kim

Abstract. **We consider different mechanisms of nonlinear frequency up-conversion of femtosecond pulses emitted by an erbium fibre system (λ = 1.5 μm) to the range of 0.8–1.2 μm in nonlinear silica fibres. The generation efficiency and the centre frequencies of dispersive waves are found as functions of the parameters of the fibre and the input pulse. Simple analytical estimates are obtained for the spectral distribution of the intensity and the frequency shift of a wave packet in the region of normal dispersion during the emission of a high-order soliton under phase matching conditions. In the geometrical optics approximation the frequency shifts are estimated in the interaction of dispersive waves with solitons in various regimes.**

Keywords: *wave dispersion, nonlinear fibre optics, seed pulses for parametric amplification, interaction of solitons and dispersive waves.*

1. Introduction

One of the important methods for obtaining ultrahigh optical fields relies on the use of optical parametric chirped-pulse amplifiers based on large-aperture DKDP crystals [1]. These amplifiers pumped by the second harmonic of a neodymium laser produce pulses at the wavelength of a signal wave $\lambda_{sn} \approx$ 0.9 μm with an energy of 25 J and a duration of 45 fs, which corresponds to the 0.56-PW pulse power [2]. Because the required radiation source emitting at the wavelength of the signal wave is not available, in the first stage of parametric amplification noncollinear phase matching was used in the interaction of the second harmonic of neodymium radiation (0.515 μm) and the idler wave from the Cr : forsterite laser (wavelength of 1.25 μm).

This paper deals with the possibility of direct ultrashort pulse generation at $\lambda_{sn} \approx 0.9$ μm. Such pulses can be generated in a nonlinear-optical converter, consisting of a segment of a highly nonlinear silica fibre. The possibility to produce ultrashort pulses in the 1-μm range using femtosecond pulses generated by an erbium-doped fibre system at a wavelength of 1.56 μm was previously shown in papers [3, 4] (see also [5]).

The most effective mechanism for producing such short-wavelength radiation is the generation of linear dispersive waves in the region of normal dispersion of an optical fibre under compression during the propagation of a high-order soliton pulse whose wavelength lies in the region of anomalous dispersion [6–10]. In view of the need to observe phase-matching conditions for their generation, one can often find the term 'Cherenkov radiation'. Ability to generate dispersive waves was especially actively investigated in relation to photonic-crystal fibres, the manufacturing technology of which allows one to form the given profile of the dispersion curve in a very wide range of wavelengths [11]. From the fundamental and applied points of view, of interest is the interaction of dispersive waves with soliton pulses, which can lead to a further increase in the frequency and mastering of even a shorter wavelength range. To date, continuous frequency tuning of dispersive waves is well studied in the interaction with a potential of a frequency-shifted Raman soliton [12–15]. In addition, using numerical simulations Liu et al. [16] found a stepwise frequency shift.

In this paper, we analyse in detail the mechanism of generation of dispersive waves by a high-order soliton and provide a simple analytical approach in the framework of geometrical optics to estimate the frequency shift of the wave packets in the region of normal dispersion during their interaction with solitons. Numerical modelling confirms a rather high accuracy of the analytical estimates. As a real system, we consider the propagation of femtosecond pulses emitted by an erbium-doped fibre laser system at a wavelength of 1.5 μm in highly nonlinear dispersion-shifted silica fibres.

It should be noted that these results can also be used to generate tunable pulses in the visible optical range in photonic crystal fibres pumped by a Ti : sapphire laser or a fibre laser near 1 μm.

2. Generation of dispersive waves in *N*the-order soliton compression

In the general case, the generation dynamics of the dispersive waves in the region of normal group velocity dispersion, and their interaction with frequency-shifted fundamental solitons or higher-order solitons in the region of anomalous dispersion can be considered within the framework of the generalised nonlinear Schrödinger equation [17]:

$$\frac{\partial A(z,\tau)}{\partial z} = \mathrm{i}\sum_{m=2}^{N}\frac{\mathrm{i}^m}{m!}\beta_m(\omega_0)\frac{\partial^m A(z,\tau)}{\partial \tau^m} + \mathrm{i}\gamma\left(1+\frac{\mathrm{i}}{\omega_0}\frac{\partial}{\partial\tau}\right)\left[A(z,\tau)\int_{-\infty}^{\infty}R(\eta)\,|A(z,\tau-\eta)|^2\,\mathrm{d}\eta\right], \quad (1)$$

where $A(z,\tau)$ is the slowly varying amplitude; z is the coordinate along the fibre axis; τ is the time in the retarded frame; β is the waveguide mode propagation constant; $\beta_m = \partial^m\beta/\partial\omega^m$; $\omega = 2\pi f$ is the angular frequency; ω_0 is the carrier frequency; γ is the nonlinearity coefficient; and $R(t)$ is the delayed (Raman) nonlinear response [17, 18].

E.A. Anashkina, A.V. Andrianov, A.V. Kim Institute of Applied Physics, Russian Academy of Sciences, ul. Ul'yanova 46, 603950 Nizhnii Novgorod, Russia; e-mail: elena.anashkina@gmail.com

Received 24 December 2012
Kvantovaya Elektronika **43** (3) 263–270 (2013)
Translated by I.A. Ulitkin

Equation (1) can be numerically integrated by the pseudo-spectral split-step Fourier method (SSFM) [17]; the results of the integration will be presented in Section 4. For qualitative understanding of the properties and analytical estimates we will consider first a simplified model that takes into account the Kerr nonlinearity as well as quadratic and cubic dispersions

$$\frac{\partial A(z,\tau)}{\partial z} + \mathrm{i}\frac{B_2}{2}\frac{\partial^2 A(z,\tau)}{\partial \tau^2} - \frac{B_3}{6}\frac{\partial^3 A(z,\tau)}{\partial \tau^3} + \mathrm{i}\gamma|A(z,\tau)|^2 A(z,\tau) = 0, \quad (2)$$

where $B_2 = \beta_2(\omega_0)$, $B_3 = \beta_3(\omega_0)$. Equation (2) describes both the radiation of dispersive waves and their interaction with the soliton pulses.

Consider the initial stage of the evolution of the Nth-order soliton pulse [$N = (\gamma P_0 t_0^2/|\beta_2|)^{1/2}$] [17], given in the region of anomalous dispersion of a nonlinear optical fibre. Due to self-phase modulation the spectrum is broadened. When the phase-matching point is reached by the high-frequency wing in the region of normal dispersion, radiation of dispersive waves starts [8–10].

Figure 1 shows the propagation of the pulse with the initial amplitude $A(0,\tau) = \sqrt{P_0}/\cosh(\tau/t_0)$, $t_0 = 20$ fs (corresponding to the full width half maximum duration $T_{\mathrm{FWHM}} = 35$ fs), $N = 2.5$ and the initial spectrum (Fig. 1a) in a fibre with the propagation constant β, its first $\beta_1 = 1/V_{\mathrm{gr}}$ and second β_2 derivatives presented in Figs 1b, c and a, respectively. The signal spectra for different z are shown in Fig. 1d. Figure 1e shows the time dependence of the femtosecond signal intensity for $z = 6L_{\mathrm{NL}}$, where the nonlinear length $L_{\mathrm{NL}} = 1/(\gamma P_0)$ and P_0 is the peak power. At the trailing edge of the soliton (Fig. 1e), one can clearly see the short-wavelength (SW) pulse.

For applications, of interest is the generation of such SW pulses at some centre frequency. In order to optimise the process, by solving numerically equation (2), we studied the dependence of the output frequency and efficiency (the ratio of the energy in the first SW pulse to the energy of the input Nth-order soliton) on B_3 and N for fixed B_2, γ and t_0. Contour curves in Fig. 2a show the frequency shift, f, in the THz range, corresponding to a shift of the maximum of the SW pulse spectrum with respect to the input frequency of the Nth-order soliton. Contour curves in Fig. 2b show the efficiency of generation at different N. Note that at $N > 2$ the soliton can emit several wave packets in the region of normal dispersion with some time delays [19]. We traced the first emitted wave packet (though its spectrum may overlap with the second and subsequent wave packets). The closer the zero-dispersion wavelength to the input wavelength of the initial soliton (the higher the value of B_3 at a fixed B_2), the lower the frequency of the wave packet in the region of normal dispersion and the higher the efficiency for fixed N. For large N with fixed B_3, higher-frequency pulses can be generated. As follows from Fig. 2, for the erbium-doped laser system, emitting near 1.5 μm (200 THz), one can obtain pulses at wavelengths of less than 0.9 μm (200 + 140 = 340 THz) to 1.2 μm (250 THz) with an efficiency of 10%–20%.

It should be noted that the obtained efficiencies are generally consistent with the results of papers [20, 21]. However, Chang et al. [21] showed that under pumping by few-cycle pulses whose spectrum was originally part of the region of normal dispersion, it is possible to obtain dispersive waves with 35% efficiency.

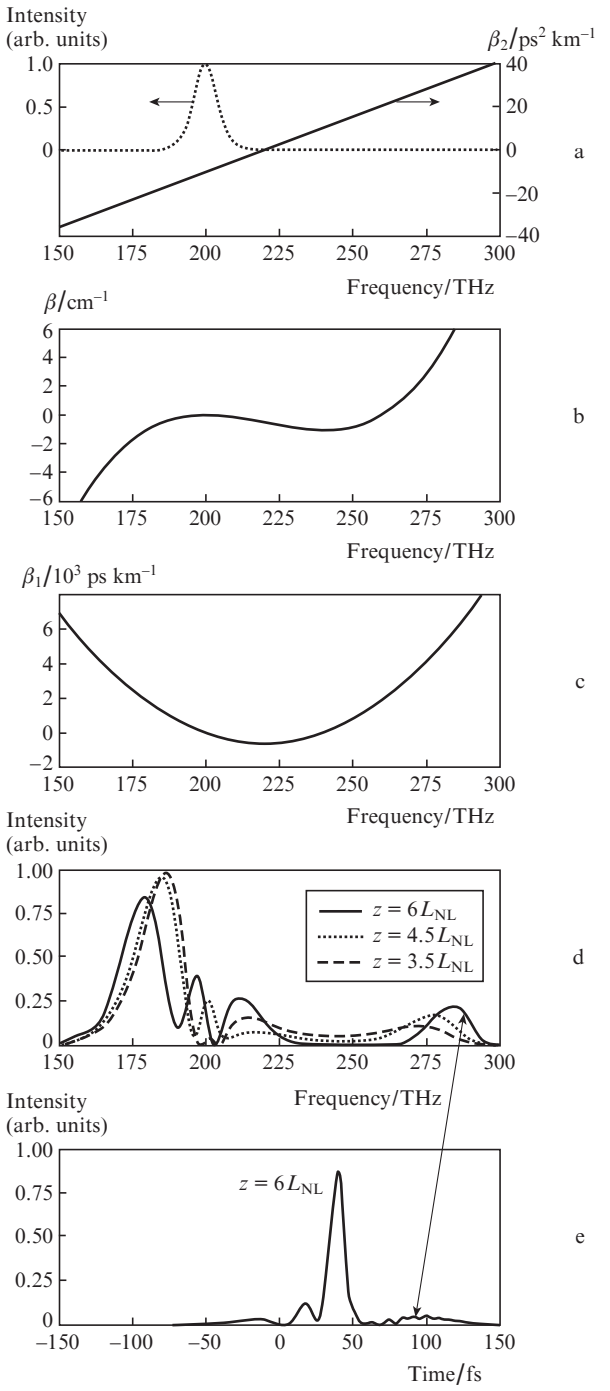

Figure 1. (a) Spectrum of the input pulse and model dispersion curve of the fibre; (b) propagation constant of the waveguide mode β and (c) its derivative; (d) spectrum of the signal at various lengths of the fibre; and (e) temporal distribution of the signal intensity. Double arrow in Figs 1d and e shows the correspondence between the spectrum of the SW pulse and its location on the time axis.

Let us now consider in more detail the initial stage of the process of dispersive wave emission by a high-order soliton within the framework of a simple model based on equation (2).

We represent the solution in the form $A = A_{\mathrm{S}} + A_{\mathrm{DW}}$, where the small addition A_{DW} corresponds to radiating dispersive waves, while A_{S} is responsible for the soliton component. In the first approximation in A_{DW} the right-hand side of the equation takes the form $|A_{\mathrm{S}}|^2 A_{\mathrm{S}} + 2|A_{\mathrm{S}}|^2 A_{\mathrm{DW}} + A_{\mathrm{S}}^2 A_{\mathrm{DW}}^*$. The term $|A_{\mathrm{S}}|^2 A_{\mathrm{S}}$ describes the soliton source, generating a

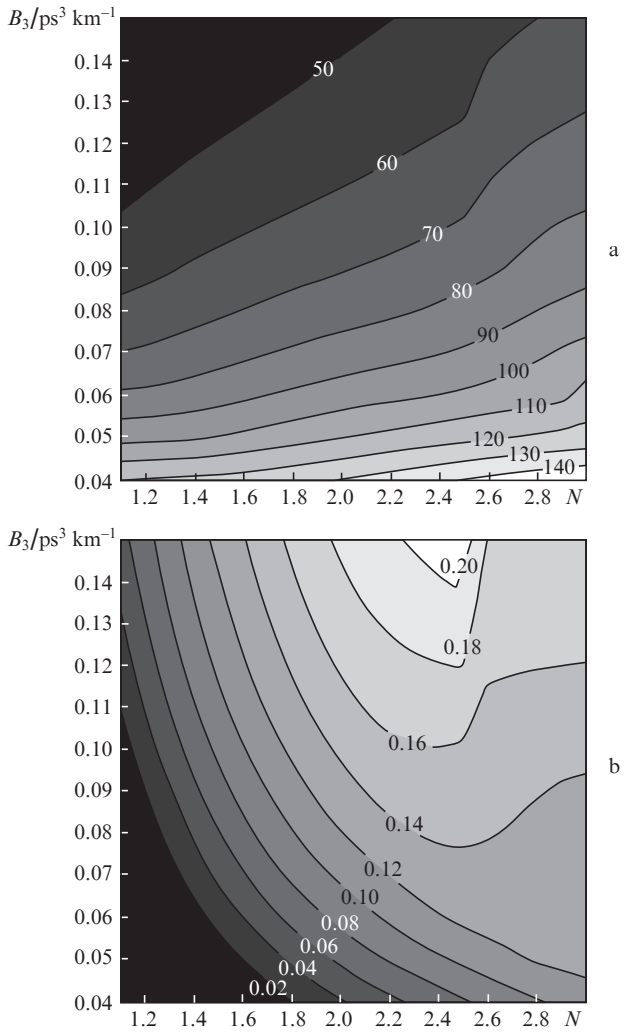

Figure 2. (a) Frequency difference f (in THz) of the first wave packet generated in the region of normal dispersion and the initial frequency of the Nth-order soliton and (b) generation efficiency of dispersive waves.

wace packet of dispersive waves, the other terms being responsible for the dynamics of the wave packet of dispersive waves propagating in the potential of the soliton.

We write the equation (2) in terms of the Fourier transforms, taking into account only the soliton source in the right-hand side:

$$\frac{\mathrm{d}F}{\mathrm{d}z} = \mathrm{i}\beta(\omega)F + \mathrm{i}\gamma Q_\mathrm{S}(\omega, z), \tag{3}$$

where

$$F = \frac{1}{2\pi}\int_{-\infty}^{\infty} A(t)\exp(\mathrm{i}\omega t)\,\mathrm{d}t,$$

$$Q_\mathrm{S} = \frac{1}{2\pi}\int_{-\infty}^{\infty} |A_\mathrm{S}|^2 A_\mathrm{S}\exp(\mathrm{i}\omega t)\,\mathrm{d}t.$$

The initial stage of generation of a wave packet of dispersive waves can be investigated without taking into account the linear in A_DW terms in right-hand side. Because the dispersive waves are generated in a fairly narrow frequency band, it is enough to know the Fourier spectrum of the source $Q_\mathrm{S}(\omega, z)$ only near the phase-matching frequency. In addition, the numerical simulation shows that the dispersive waves are generated only in a sufficiently narrow interval of the propagation coordinate z: from $z_\mathrm{DW} - \delta z$ to $z_\mathrm{DW} + \delta z$.

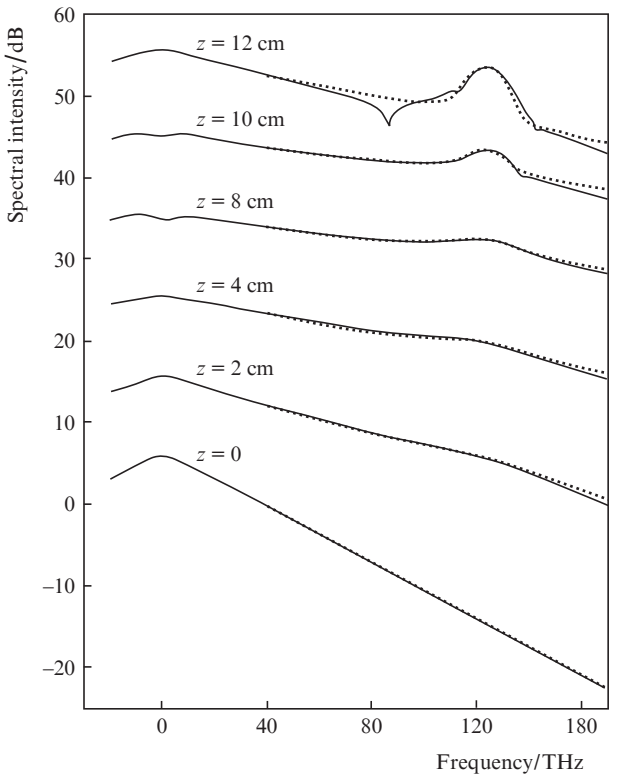

Figure 3. Shift of the SW wing of the spectrum (in a logarithmic scale) during the propagation of a second-order soliton in a fibre with cubic dispersion ($\beta_3 = 0.04$ ps^3 km^{-1}), obtained by numerical simulation (solid lines) and with the approximate analytical solutions, constructed by formula (6) (points). For convenience, each curve is shifted by 10 dB with respect to the previous one.

A detailed study of the results of numerical simulations allows us to find a simple dependence, which can approximate the function $Q_\mathrm{S}(\omega, z)$ in the region near the point $(\omega_\mathrm{DW}, z_\mathrm{DW})$. It turns out that the modulus of this function has an exponential square-law frequency dependence varying along z and the phase of this function is determined by the phase of the soliton with its group velocity taken into account:

$$Q_\mathrm{S} = q\exp[-a\omega(z - z_\mathrm{DW})^2 - b\omega + \mathrm{i}\beta_\mathrm{S} z], \tag{4}$$

where q, a and b are the constants.

The soliton propagation constant at a frequency ω_S can be approximately written as

$$\beta_\mathrm{S} = \beta_0(\omega_\mathrm{S}) + \beta_1(\omega_\mathrm{S})(\omega - \omega_\mathrm{S}) + \gamma P_0/2. \tag{5}$$

Then the solution of the linear equation (3) can be expressed as

$$F = \frac{\mathrm{i}\gamma q\sqrt{\pi}}{2\sqrt{a\omega}}\exp\left[-\frac{[\beta(\omega) - \beta_\mathrm{S}]^2}{4a\omega} - b\omega - \mathrm{i}\beta(\omega)z\right]$$

$$\times\left\{1 - \mathrm{erf}\left[\frac{\mathrm{i}[\beta(\omega) - \beta_\mathrm{S}]}{2\sqrt{a\omega}} - \sqrt{a\omega}\,(z - z_\mathrm{DW})\right]\right\}. \tag{6}$$

A rather complicated solution makes it impossible to instantly identify its properties, but allows one to verify the adequacy of the approximations made in comparison with the numerical simulations. Figure 3 shows the results of numerical

simulations and the analytical solution by formula (6). One can see that the analytical solution reproduces well the exponential wing of the soliton pulse and the appearance of a nearly Gaussian spectral peak of dispersive waves, corresponding to the phase-matching condition $\beta(\omega) - \beta_S = 0$.

Being interested only in the value of $|F|^2$ at the phase-matching frequency, we can use equation (6) to derive the expression:

$$|F(\omega_{DW})|^2 = \frac{\pi\gamma^2 q^2}{4a\omega_{DW}} \exp(-2b\omega_{DW}) \times \{1 + \mathrm{erf}[\sqrt{a\omega_{DW}}\,(z - z_{DW})]\}^2, \quad (7)$$

which shows how the spectral peak intensity of the dispersive waves increases during emission. The position of the phase-matching point, generally speaking, is displaced during emission by changing the centre frequency of the soliton and its peak intensity. Because these changes are much smaller than the value of ω_{DW} and occur gradually, the constructed solution remains approximately correct if ω_{DW} is considered to be a function, which is weakly dependent on z. It should be noted that in accordance with the approximations the constructed solution does not take into account the dynamics of the emerging dispersive wave packet in the soliton field, which leads to a shift of the maximum of the spectral peak in the output signal. The interaction of the dispersive waves with the refractive index changes induced by the soliton will be investigated elsewhere.

At this stage, by neglecting the above-mentioned corrections, we can simplify the expression for $|F|^2$ in the case of large z, where the radiation process has already terminated. Then, using the explicit form of the dispersion dependence and neglecting the correction to the phase-matching condition related to the pulse power, we can show that the emission spectrum of the dispersive waves is approximately Gaussian:

$$|F|^2 = \frac{\pi\gamma^2 q^2}{4a\omega} \exp\left(-\frac{[\beta(\omega) - \beta_S]^2}{2a\omega} - 2b\omega\right) \approx \frac{\pi\gamma^2 q^2}{4a\omega} \exp\left(-\frac{(\omega - \omega_{DW})^2}{\Delta\omega^2} - 2b\omega_{DW}\right). \quad (8)$$

The width of the resulting peak of the dispersive waves is

$$\Delta\omega \approx \frac{8\sqrt{2a\omega_{DW}}\,\beta_3}{3(\beta_2 + \beta_3\omega_{DW})^2}. \quad (9)$$

As seen from expressions (6)–(9), an important feature of the dispersive wave generation by higher-order solitons is the dependence of the intensity and width of the emitted spectrum on the speed with which the soliton parameters change during its initial compression. Figure 4 shows the dependence of the width of the spectral peak of the dispersive waves on the order of the input soliton for fixed dispersion.

We now consider the mechanism of interaction of the dispersion waves with the Nth-order soliton. As can be seen from Fig. 1d, in the course of radiation by solitons the centre frequency of the pulse rises smoothly in the region of normal dispersion. This phenomenon is due to two effects: first, the above-discussed change in the position of the phase-matching point, and second, the interaction with the soliton as a result of cross-phase modulation.

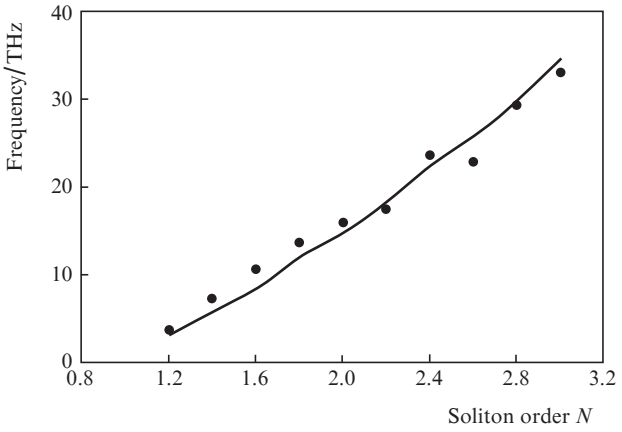

Figure 4. Dependence of the spectral peak width of the dispersive waves on the order of the input soliton, obtained by numerical simulation of equation (2) (points) and constructed by formula (9) (solid line).

To study analytically the interaction, the well-known geometrical optics approach can be well applied, naturally assuming that, first, the peak power of the SW pulse is much less than the power of the soliton, which allows one to neglect the reverse effect of the dispersive waves on the soliton itself, and second, the nonlinear length for the SW pulse is much larger than the interaction length with the soliton, which permits the use of a linear approximation for the dispersive waves. In this case, the Hamiltonian H of the SW pulse propagating in a fibre with a refractive index induced by the soliton can be written as [22]:

$$H = \left(\frac{\partial\varphi}{\partial z}\right)^2 - k_0^2 n_{eff}^2 = 0. \quad (10)$$

Here φ is the phase; z is the coordinate along the fibre; n_{eff} is the effective refractive index; k_0 is the wave number in a vacuum; and

$$k_0^2 n_{eff}^2 = (\beta + \gamma|U|^2)^2, \quad (11)$$

where $U(t)$ is the known slow envelope of the soliton pulse field.

The eikonal equation (10), a nonlinear partial differential first-order equation, belongs to a class of Hamilton–Jacobi equations and can be solved by the method of characteristics [22].

The equation of characteristics can be written in a canonical Hamiltonian form:

$$\frac{\partial z}{\partial\xi} = \frac{\partial H}{\partial k}, \quad (12)$$

$$\frac{\partial k}{\partial\xi} = -\frac{\partial H}{\partial z}, \quad (13)$$

$$\frac{\partial t}{\partial\xi} = -\frac{\partial H}{\partial\omega}, \quad (14)$$

$$\frac{\partial\omega}{\partial\xi} = \frac{\partial H}{\partial t}, \quad (15)$$

where k is the effective wave number; $H = H(\omega, k, z)$ is the Hamiltonian given by expressions (10) and (11); and ξ is the parameter that varies along the characteristic.

The solution $\{t(\xi), z(\xi)\}$ of Eqns (12)–(15) defines the space–time rays in the two-dimensional space $\{t, z\}$, which can be regarded as a projection of the four-phase trajectory $\{t(\xi), z(\xi), \omega(\xi), k(\xi)\}$, satisfying the system of equations (12)–(15), onto the two-dimensional space $\{t(\xi), z(\xi)\}$.

The equations of space–time rays (12)–(15) can be represented [22] in the form:

$$\frac{\partial t}{\partial z} = \frac{\partial H/\partial \omega}{\partial H/\partial k}, \tag{16}$$

$$\frac{\partial \omega}{\partial z} = \frac{\partial H/\partial t}{\partial H/\partial k}, \tag{17}$$

$$\frac{\partial k}{\partial z} = \frac{\partial H/\partial z}{\partial H/\partial k}, \tag{18}$$

and then with (10) and (11) taken into account transformed to the form

$$\frac{\partial t}{\partial z} = \frac{\partial \beta}{\partial \omega}, \tag{19}$$

$$\frac{\partial \omega}{\partial z} = -\gamma \frac{\partial |U|^2}{\partial t}, \tag{20}$$

$$\frac{\partial k}{\partial z} = \gamma \frac{\partial |U|^2}{\partial z}. \tag{21}$$

It follows from equation (20) that the frequency of the SW pulse will decrease during its interaction at the rising edge of the Nth-order soliton, whereas during the interaction at the trailing edge – increase. Note the analogy of the 'fibre' problem with the famous 'plasma' problem in which a quasi-soliton signal during the interaction with the wave of medium parameters, travelling at a constant speed, can be reflected with increasing frequency [23].

Since the group velocity of the generated dispersive waves in the optical fibre with a single point of zero dispersion is less than the velocity of the soliton (Figs 1b and c), we can propose the following scenario of the SW pulse formation: first, due to Cherenkov radiation it is generated in the region of soliton localisation, and second, during the interaction with the soliton 'moves down' from it with increasing frequency according to equation (20). We assume that during the interaction the centre frequency of the Nth-order soliton has no time to change, and the group velocity is constant. Then, integrating (20), (21) with the condition $|U|^2 = |U(z - V_{gr}t)|^2$ taken into account, we obtain

$$\omega - kV_{gr} = \text{const}. \tag{22}$$

The Nth-order soliton begins to emit near the point of maximum compression, z, with a peak power P_{max}, whose dependence on the distance along the fibre is shown in Fig. 5a. Figure 5b shows the frequency corresponding to the maximum of the wave packet spectrum in the region of normal dispersion.

First let dispersive waves be emitted at the centre frequency ω_1, and after the 'recession' of the waves over time due to the difference of the group velocities the frequency shifts to ω_2. We assume that the SW pulse begins to form in the time representation near the peak power of the soliton, P_{max}. Then from (22) with (11) taken into account, we have

$$\omega_1 - V_{gr}[\beta(\omega_1) + \gamma P_{max}] = \omega_2 - V_{gr}\beta(\omega_2). \tag{23}$$

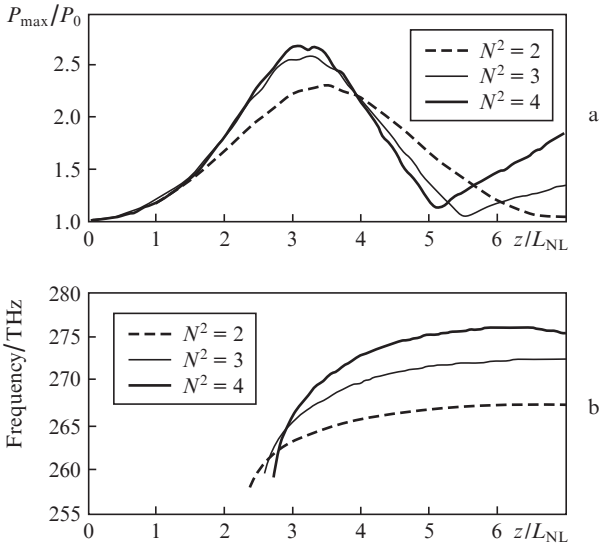

Figure 5. (a) Peak power of the Nth-order soliton and (b) frequency corresponding to the maximum of the wave packet spectrum in the region of normal dispersion as functions of the fibre length for different N.

From whence we immediately obtain an estimate for the frequency shift ($\omega_2 - \omega_1 \ll \omega_1$), which is valid for the dispersion curve of any profile:

$$\omega_2 - \omega_1 \approx \frac{\gamma P_{max}}{\beta_1(\omega_1) - \beta_1(\omega_S)}. \tag{24}$$

If we take into account only the quadratic and cubic dispersions and neglect under phase-matching conditions the term $\gamma P_0/2$ in the right-hand side of (5), it turns out that the initial frequency of the dispersive waves is $\omega_1 \approx 3B_2/B_3$. In this case, equation (24) takes a very simple form:

$$\omega_2 - \omega_1 \approx \frac{2}{3}\frac{\gamma P_{max} B_3}{B_2^2}. \tag{25}$$

At not very large N ($N < 2.5$) to estimate the order of the spectral shift, use can be made of the expression

$$\omega_2 - \omega_1 \approx \frac{2\gamma P_0 B_3}{B_2^2}. \tag{26}$$

Figure 6 shows a good correlation between the dependence of the frequency shift of the wave packet in the region

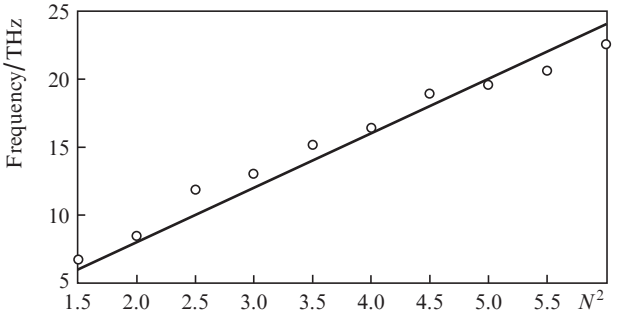

Figure 6. Difference between the carrier frequencies of the dispersive waves Δf after their interaction with the soliton and the start of radiation, obtained by numerical simulation (points) and by formula (26) (solid line).

of normal dispersion on N^2, found in the numerical solution of equation (2), and the dependence, constructed by formula (26), where the notation $\Delta f = (\omega_2 - \omega_1)/(2\pi)$ is introduced.

3. 'Collision' of dispersive waves with a fundamental soliton

It is interesting to note that the process of radiation and interaction of the dispersive waves can be repeated many times for the high-order soliton. As is known, the pump pulse demonstrates fission into fundamental solitons and the same number of relevant SW pulses, which then propagate at a constant group velocity [19]. In this case, the velocity of the solitons in the fibre decreases due to a decrease in the carrier frequency as a result of the Raman scattering [17, 18].

We consider a low-frequency fundamental soliton and the first emitted SW pulse, which falls behind the soliton. When propagating in the fibre, the soliton can slow down so that SW pulse catches it up, and the interaction may occur at the trailing edge [21], which can be conveniently interpreted as a collision. From (22), assuming the group velocity of the soliton to be constant during the interaction with the SW pulse, follows the condition relating the centre frequencies of the latter before and after the collision:

$$\beta(\omega_1)V_{gr} - \omega_1 = \beta(\omega_2)V_{gr} - \omega_2, \tag{27}$$

whence at $\omega_2 - \omega_1 \ll \omega_1$ we obtain that

$$\omega_2 - \omega_1 \approx \frac{2[\beta_1(\omega_S) - \beta_1(\omega_1)]}{\beta_2(\omega_1)}. \tag{28}$$

If we take into account only the quadratic and cubic dispersions, expression (28) transforms to the form that does not depend on the slope of the dispersion curve:

$$\omega_2 - \omega_1 \approx \frac{(\omega_S - \omega_{ZD})^2 - (\omega_1 - \omega_{ZD})^2}{\omega_1 - \omega_{ZD}}, \tag{29}$$

where ω_{ZD} is the wavelength of the zero group velocity dispersion.

Figure 7a shows the numerical solution of equation (2) for the spectrum evolution as the pulse propagates along the fibre. At $z < 6$ cm the SW pulse (*1*) catches up with the soliton, and at 6 cm $< z <$ 10 cm they start to interact. Then, part of the wave packet (*2*) is reflected with increasing frequency, and part of it (*3*) propagates without any change in its frequency. The temporal distribution of the pulse intensity at $z = 0$ and $z = 20$ cm for the same parameters is shown in Fig. 7b.

After collision the SW pulse has a lower velocity than the soliton. If the fibre is sufficiently long, the soliton can slow down again due to the Raman frequency shift [neglected in equation (*2*), but described by equation (*1*)], so that the SW pulse can catch up with it and collide again with increasing frequency. This process can occur more than once [16].

The collision regime can also be implemented if, immediately after the formation of the SW pulse and the fundamental soliton, the first nonlinear optical fibre is connected to the second nonlinear optical fibre, in which the soliton propagates with a slower group velocity than the pulse in the region of normal dispersion. This regime can be used in applications, requiring optically synchronised pulses at different frequencies, and to expand the boundaries of the supercontinuum.

It should be noted that in the geometrical optics model it is impossible to calculate the reflectivity of the SW signal;

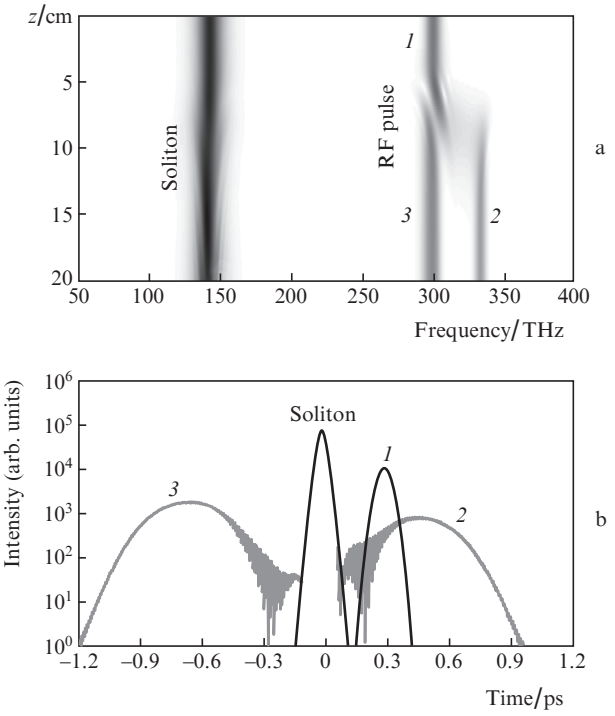

Figure 7. (a) Spectral evolution of the signal during its propagation in the fibre and (b) temporal distribution of the signal intensity at the input of the fibre (black curves) and at a distance of 20 cm (gray curves): (*1*) SW pulse before interaction with the soliton, (*2*) reflected pulse, (*3*) propagated pulse. Simulation parameters: $B_2 = -10$ ps^2 km^{-1}, $B_3 = -0.08$ ps^3 km^{-1}, $N = 2.5$.

however, one can estimate the frequency shift with good accuracy. Calculations show that at the same soliton frequency and the same initial pulse frequency the shift in the region of normal dispersion is independent of B_3, which is consistent with (29). If we introduce the notations $x = (\omega_S - \omega_{ZD})/(\omega_1 - \omega_{ZD})$, $y = (\omega_2 - \omega_1)/(\omega_1 - \omega_{ZD})$, then (29) takes the form

$$y = x^2 - 1. \tag{30}$$

Figure 8 shows the graph of the function $y(x)$, given by (30), and the estimated value of the function $y(x)$, found in the numerical integration of equation (2). By $\omega_{1,2}$ are meant

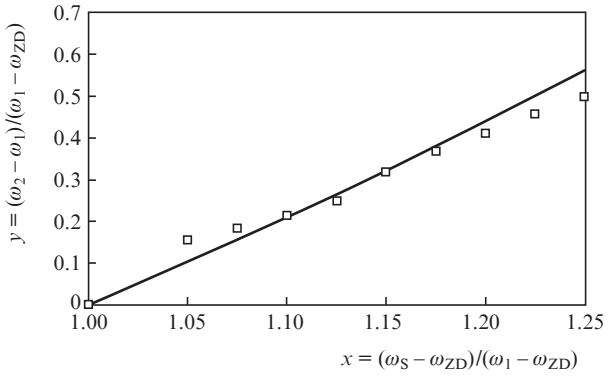

Figure 8. Dependence of the frequency shift of the wave packet in the region of normal dispersion regime in the regime of a collision with the soliton, obtained by numerical simulation (squares) and constructed by analytical formula (30) (solid line).

the frequencies corresponding to the maxima of the spectra of the corresponding wave packets. At relatively small values of x the spectra of the wave packets are overlapped, and at relatively large x the assumption $\omega_2 - \omega_1 \ll \omega_1$ is violated; therefore, the calculated and theoretical values differ slightly. At intermediate values of x, formula (30) and numerical simulations coincide with a good degree of accuracy.

4. Quasi-continuous interaction of dispersive waves with a Raman soliton

We have considered above the interaction of SW pulses with a soliton in the form of a collision, which can be repeated many times in sufficiently long fibres. However, it is clear that at certain velocities of the Raman frequency shift of the soliton, the frequency of the SW pulse can increase continuously. In this case, the latter is captured by a decelerating soliton, thereby increasing its frequency in accordance with the rate of deceleration [12–15], so that the group velocity of the SW pulse and the velocity of the soliton remain locally identical. This case of group phase-matching can also be easily analysed in the framework of the geometrical optics.

For maximum frequency tuning of the SW pulse it is desirable to make use of a fibre with the most flat spectral dependence of normal dispersion. Then, while maintaining the group phase-matching conditions, the rate of the SW signal shift is higher than the rate of the frequency shift of the soliton. The limiting frequency $\omega_1^{\max}$, to which the SW pulse can be tuned, is estimated from the condition $\beta_1(\omega_1^{\max}) = \beta_1(\omega_S^{\min})$, where $\omega_S^{\min}$ is the minimum achievable frequency of the Raman soliton during its propagation in a nonlinear fibre. This frequency is mainly determined by the loss of the fibre and to a lesser degree by the soliton energy. For example, in germanosilicate fibres solitons can be produced at wavelengths of up to 2.5 μm [24], which theoretically allows one to estimate the minimum wavelength of the SW pulses in these fibres to be less than 0.8 μm.

A situation is also possible, in which the chirped SW pulse in a collision with a soliton begins to increase abruptly the frequency at the leading edge, but the 'new' frequency is already present in its spectrum, i.e., a continuous frequency shift can occur as a result of extended collisions of the SW pulse leading edge with the soliton trailing edge.

For a quantitative analysis we will use equation (1). To analyse the position of different spectral components on the time axis we construct a spectrogram

$$S(\omega,\tau) = \left| \int A(t) w(t-\tau) \exp(-\mathrm{i}\omega t)\, \mathrm{d}t \right|, \qquad (31)$$

where $w(t) = \exp[-(t/T)^2]$ is the window function ($T = 20$ fs). Figure 9 demonstrates the function $S(\omega,\tau)$ [calculated by (31)], constructed at various points in the fibre. Figure 9a shows a situation when the SW pulse (*1*) is behind the soliton. Figure 9b shows a situation when part of the wave packet (*3*) has passed through the soliton without changing the frequency, part (*2*) has been reflected with increasing frequency, and part (*1*) has not yet interacted. Figure 9c shows a case when almost the entire original wave packet has already interacted. It should be noted that the figure similar to Fig. 9b has been published previously [25]; however, the authors presented the results without comments.

5. Conclusions

We have considered the radiation of the dispersion waves by high-order soliton pulses in nonlinear silica fibres. It is shown that when the generation efficiency of the pulses in the region of normal dispersion is 10%–20%, wavelength tuning range of 0.8–1.2 μm becomes available. We have considered the following regimes of increasing the dispersive wave frequency in the interaction with optical solitons in nonlinear optical fibres: 'sliding down' from the trailing edge of the soliton, reflection and quasi-synchronous interaction with the Raman soliton. As a part of the geometrical optics approach, we have obtained simple estimates of changes in the frequency, which are in good agreement with numerical simulations.

Acknowledgements. The work was supported by the programme 'Extreme Light Fields and Their Applications' of the Presidium of RAS, the Russian Foundation for Basic Research (Grant Nos 12-02-31344, 12-02-33074 and 12-02-

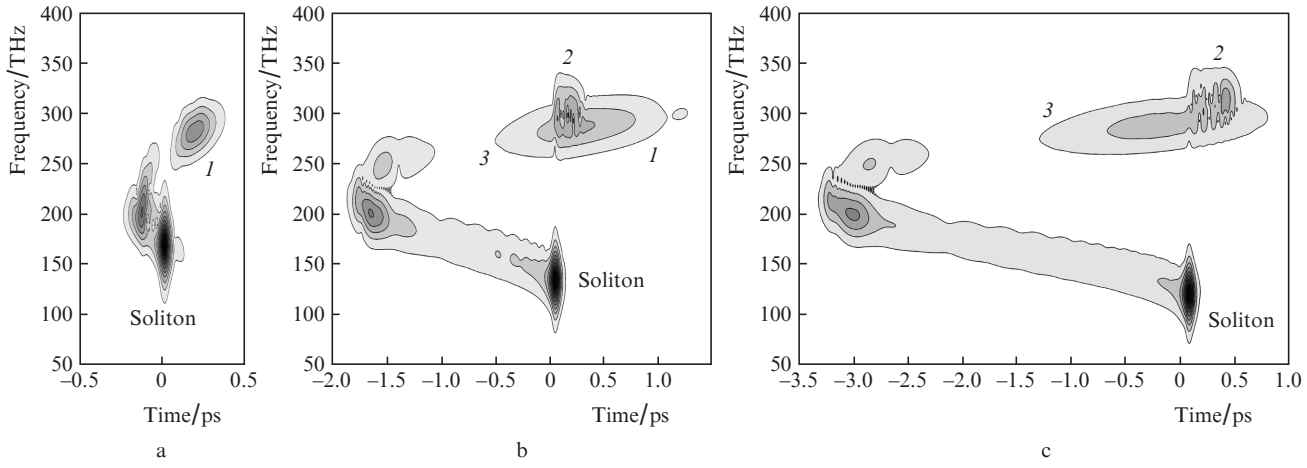

Figure 9. Spectrograms of the optical signal at the output of the nonlinear fibre at (a) $z = 12L_{NL}$, (b) $50L_{NL}$ and (c) $70L_{NL}$: (*1*) SW pulse before interaction with the soliton, (*2*) reflected pulse, (*3*) propagated pulse. Simulation parameters: $B_2 = -10$ ps^2 km^{-1}, $B_3 = -0.07$ ps^3 km^{-1}, $B_4 = 6\times10^{-5}$ ps^4 km^{-1}, $N = 2.5$.

12101) and the Russian Ministry of Education (State Agreement 14.132.21.1433, 8626). E.A. Anashkina expresses her gratitude to the non-profit Dynasty Foundation for financial support under the grant for post-graduate students and young scientists without a degree.

References

1. Korzhimanov A.V., Gonoskov A.A., Khazanov E.A., Sergeev A.M. *Usp. Fiz. Nauk*, **181**, 9 (2011).
2. Lozhkarev V.V., Freidman G.I., Ginzburg V.N., Katin E.V., Khazanov E.A., Kirsanov A.V., Luchinin G.A., Mal'shakov A.N., Martyanov M.A., Palashov O.V., Poteomkin A.K., Sergeev A.M., Shaykin A.A., Yakovlev I.V. *Laser Phys. Lett*., **4**, 421 (2007).
3. Andrianov A.V., Anashkina E.A., Muraviov S.V., Kim A.V. *Opt. Lett*., **35**, 3805 (2010).
4. Kieu K., Jones R.J., Peyghambarian N. *Opt. Express*, **18**, 21350 (2010).
5. Andrianov A.V., Anashkina E.A., Murav'ev S.V., Kim A.V. *Kvantovaya Elektron*., **43**, 256 (2013) [*Quantum Electron*., **43**, 256 (2013)].
6. Wai P.K.A., Menyuk C.R., Lee Y.C., Chen H.H. *Opt. Lett*., **11**, 464 (1986).
7. Wai P.K.A., Chen H.H., Lee Y.C. *Phys. Rev. A*, **41**, 426 (1990).
8. Karpman V.I. *Phys. Rev. E*, **47**, 2073 (1993).
9. Akhmediev N., Karlsson M. *Phys. Rev. A*, **51**, 2602 (1995).
10. Elgin J.N., Brabec T., Kelly S.M.J. *Opt. Commun.*, **114**, 321 (1995).
11. Saitoh K., Koshiba M., Hasegawa T., Sasaoka E. *Opt. Express*, **11**, 843 (2003).
12. Skryabin D.V., Yulin A.V. *Phys. Rev. E*, **72**, 016619 (2005).
13. Gorbach A.V., Skryabin D.V. *Nat. Photon.*, **1**, 653 (2007).
14. Judge A.C., Bang O., de Sterke C.M. *J. Opt. Soc. Am. B*, **27**, 2195 (2010).
15. Liu H., Dai Y., Xu C., Wu J., Xu K., Li Y., Hong X., Lin J. *Opt. Lett.*, **35**, 4042 (2010).
16. Liu C., Rees E.J., Laurila T., Jian S., Kaminski C.F. *Opt. Express*, **20**, 6316 (2012).
17. Agrawal G.P. *Nonlinear Fiber Optics* (Boston: Acad. Press, 2007).
18. Blow K.J., Wood D. *IEEE J. Quantum Electron.*, **25**, 2665 (1989).
19. Husakou A.V., Herrmann J. *Phys. Rev. Lett*., **87**, 203901 (2001).
20. Roy S., Bhadra S.K., Agrawal G.P. *Phys. Rev. A*, **79**, 023824 (2009).
21. Chang G., Chen L.-J., Kärtner F.X. *Opt. Express*, **19**, 6635 (2011).
22. Kravtsov Yu.A., Orlov Yu.I. *Geometrical Optics of Inhomogeneous Media* (Berlin: Springer-Verlag, 1990; Moscow: Nauka, 1980).
23. Vanin E.V., Smirnov A.I. *Zh. Eksp. Teor. Fiz.*, **110**, 1136 (1996).
24. Anashkina E.A., Andrianov A.V., Koptev M.Yu., Mashinsky V.M., Muravyev S.V., Kim A.V. *Opt. Express*, **20**, 27102 (2012).
25. Dudley J., Gu X., Xu L., Kimmel M., Zeek E., O'Shea P., Trebino R., Coen S., Windeler R.S. *Opt. Express*, **10**, 1215 (2002).